

NASA/RSS SMAP Salinity: Version 3.0 Validated Release

Release Notes

Algorithm Theoretical Basis Document (ATBD)

Validation

Data Format Specification

Thomas Meissner, Frank Wentz and Andrew Manaster
Remote Sensing Systems, Santa Rosa, CA

Remote Sensing Systems

444 Tenth Street, Suite 200, Santa Rosa, CA 95401



(707) 545-2904

Table of Contents

1. OVERVIEW OF V3.0 RELEASE	6
1.1 Release Date	6
1.2 Data Access	6
1.3 Citation and DOI	6
1.4 Summary of Updates and Improvements from V2.0	6
1.5 Latency	7
1.6 Spatial Resolution	7
1.7 Known Issues	7
2. LEVEL 2 PROCESSING	8
2.1 Input	8
2.2 Optimum Interpolation (OI) onto Fixed Earth Grid (L2A)	8
2.3 Ancillary Fields (L2B)	8
2.4 Salinity Retrieval (L2C)	9
3. SMAP SALINITY RETRIEVAL ALGORITHM	10
3.1 Overview and Basic Flow	10
3.2 Surface Roughness Correction	10
3.2.1 Ancillary Input for Wind Speed and Direction	10
3.2.2 Wind Induced Emissivity Model	11
3.3 Correction for Emissive SMAP Antenna	12
3.4 Atmospheric Oxygen Absorption	15
3.5 IMERG Rain Rate and Correction for Liquid Cloud Water Absorption	15
3.6 Correction for Reflected Galaxy	15
3.7 Land Correction	15
3.7.1 Computation of the SMAP V3 Land Correction	15
3.7.2 Results and Performance of Land Correction	16
3.8 Antenna Pattern Correction (APC)	17

3.9	Ocean Target Calibration	18
3.10	Quality Control (Q/C) Flag	19
4.	LEVEL 3 PROCESSING	20
4.1	Standard Product	20
4.2	Rain Filtered (RF) Product	20
5.	PERFORMANCE ESTIMATE AND VALIDATION	21
5.1	Spatial Resolution and Noise Figures	21
5.2	Time Series of SMAP – ARGO – HYCOM Comparisons	21
5.3	Zonal and Average Regional Biases	23
6.	REFERENCES	25
7.	DATA FORMAT SPECIFICATION	26
7.1	Level 2C	26
7.1.1	Paths and Filenames	26
7.1.2	Global Attributes	26
7.1.3	Gridding and Dimensions	26
7.1.4	Variables	27
7.2	Level 3	29
7.2.1	Paths and Filenames	29
7.2.2	Global Attributes	30
7.2.3	Grid and Dimensions	30
7.2.4	Variables	30

List of Figures

Figure 1: Flow diagram of the SMAP salinity retrieval algorithm.10

Figure 2: Left: Isotropic (wind-direction independent) part of the wind induced emissivity that is used in the Aquarius Version 5 after interpolating to the SMAP Earth Incidence Angle (dashed lines) and the SMAP Version 3 (full lines) releases. Blue: V-pol. Red: H-pol. The figure shows the 0th harmonic of the wind induced excess emissivity (Meissner et al. 2014, 2017) multiplied by 290 K. Right: SST dependence of the wind induced emissivity for Aquarius horn 2 H-pol. The blue line is the SST dependence from Meissner et al. 2014, which is predicted by the geometric optics model for the wind induced surface emission (Meissner et al. 2012). The red line is the SST dependence used in the Aquarius Version 5 release. The green line is the SST dependence used in the SMAP Version 3 release (Meissner et al. 2018).11

Figure 3: Regression of T_A measured minus expected versus $T_{refl} - T_A$. T_{refl} is the physical temperature of the antenna. T_A is the radiometric antenna temperature. Blue: V-pol. Red: H-pol. The slope of the linear fits is the reflector emissivity.12

Figure 4: Physical temperature T_{refl} of the reflector. Left: JPL thermal model that is used in the SMAP L1B files (Piepmeier et al. 2018). Right: Empirical adjustment in the RSS SMAP Version 3 salinity release.13

Figure 5: Hovmoeller diagram of SMAP T_A measured - expected over the open ocean using the JPL thermal model for the SMAP mesh antenna. The x-axis is time (day of year) and the y-axis is orbital position (z-angle). For the computation of T_A we have used Scripps ARGO as reference salinity. The computation of this diagram is based on 2 years of SMAP data (September 2015 – August 2017). A simple spatial and temporal low-pass filter was applied by performing a running average in both dimensions.14

Figure 6: Monthly map of SSS SMAP – HYCOM for March 2018. Left: without land correction. Right: Using the V3.0 land correction.17

Figure 7: Bias (left) and standard deviation (right) of SMAP salinity retrievals versus HYCOM SSS for July 2017: blue = without any land correction, olive = using the V2.0 land correction, red = using the V3.0 land correction.17

Figure 8: Time series (APR 2015 – JUN 2018) of biases: SMAP V3 – HYCOM (blue). SMAP V3 – Scripps ARGO (red). Scripps ARGO – HYCOM (dashed black). The figure was created from the Level 3 70km rain-filtered monthly maps requiring $g_{land} < 0.001$, $g_{ice} < 0.001$, $SST > 5^\circ C$21

Figure 9: Time series (APR 2015 – JUN 2018) of standard deviations: SMAP V3 – HYCOM (blue). SMAP V3 – Scripps ARGO (red). Scripps ARGO – HYCOM (dashed black). The figure was created from the Level 3 70-km rain-filtered monthly maps requiring $g_{land} < 0.001$, $g_{ice} < 0.001$, $SST > 5^\circ C$. The green curve is the estimated RMS error in the SMAP data based on the triple collocation method.22

Figure 10: Same as Figure 9 for the 40-km product.22

Figure 11: Same as Figure 9 for 1-deg lat/lon averages.23

Figure 12: Hovmoeller diagram (APR 2015 – JUN 2018) of SMAP V3 SMAP V3 – Scripps ARGO. The figure was created from the Level 3 70km rain-filtered monthly maps requiring $g_{land} < 0.001$, $g_{ice} < 0.001$, $SST > 5^\circ C$24

Figure 13: Global map (JAN 2016 – DEC 2017) of SMAP V3 SMAP V3 – Scripps ARGO. The figure was created from the Level 3 70km rain-filtered monthly maps requiring $g_{land} < 0.001$, $g_{ice} < 0.001$, $SST > 5^\circ C$24

List of Tables

Table 1: Ancillary data sources.	8
Table 2: A-matrix elements A_{ij} (in I, Q, S3, S4 basis) of the SMAP V3 release. The entries in red denote matrix elements that differ from the pre-launch computation.	18
Table 3: 32- bit Level 2 Q/C flags in the SMAP V3.0 release.	19

1. OVERVIEW OF V3.0 RELEASE

1.1 Release Date

10/15/2018

1.2 Data Access

www.remss.com/missions/smap/

<https://podaac-opendap.jpl.nasa.gov/opendap/allData/smap/xx/RSS/V3/> xx = L2 or L3

Contact: Thomas Meissner, meissner@remss.com.

1.3 Citation and DOI

As a condition of using these data, we require you to use the following citation:

Meissner, T., F. J. Wentz, A. Manaster, 2018: Remote Sensing Systems SMAP Ocean Surface Salinities [Level 2C, Level 3 Running 8-day, Level 3 Monthly], Version 3.0 validated release. Remote Sensing Systems, Santa Rosa, CA, USA. Available online at www.remss.com/missions/smap, doi: 10.5067/xxxxxSMP30-yyyyy.

In the doi, the string xxxxx is:

1. *SMP30* for the 40km resolution products.
2. *SMP3A* for the 70km resolution products.

and the string is yyyy is:

1. *2SOCS* for the L2C files.
2. *3SPCS* for the L3 8-day running maps.
3. *3SMCS* for the L3 monthly maps.

Continued production of this data set requires support from NASA. We need you to be sure to cite these data when used in your publications so that we can demonstrate the value of this data set to the scientific community. Please include the following statement in the acknowledgement section of your paper:

"SMAP salinity data are produced by Remote Sensing Systems and sponsored by the NASA Ocean Salinity Science Team. They are available at www.remss.com."

1.4 Summary of Updates and Improvements from V2.0

1. Use of Version 4 L1B SMAP RFI filtered antenna temperatures (Piepmeier et al. 2018).
2. Use of the GMF from Aquarius Version 5 Release adapted to SMAP (Meissner et al. 2017, 2018).
 - 2.1. Use of Liebe et al. (1992) oxygen absorption model.
 - 2.2. Use of surface roughness model from Meissner et al. 2014 with the adjustments specified in Meissner et al. 2018. For deriving the adjustments, the Scripps ARGO analyzed salinity is used as reference.

- 2.3. Galactic reflection model based on SMAP fore – aft look analysis (Meissner et al. 2017, 2018).
3. Use of CCMP near real time wind speed and direction as ancillary input.
4. Inclusion of IMERG rain rate. This is used in the atmospheric liquid cloud water correction and for rain flagging.
5. Improved computation of antenna weighted land fraction g_{land} .
6. Improved correction for intrusion of land radiation from antenna sidelobes.
7. Emissive SMAP antenna:
 - 7.1. The emissivity of the mesh antenna was set to 0.01012 for both V-pol and H-pol polarizations.
 - 7.2. The empirical adjustment to the JPL thermal model was rederived using the Scripps ARGO analyzed salinity field.
8. An error in the computation of the gain-weighted sea ice fraction g_{ice} during 2017 and 2018 in V2.0 has been corrected.
9. Antenna Pattern Correction (APC): The spillover, or equivalently the matrix element A_{ij} in the APC matrix, was decreased from 1.1080 (V2.0) to 1.0929 (V3).
10. The Level 2C (quality control) flags have been updated.
- 11. The salty biases at low latitudes and the fresh biases at high N latitudes that were observed in the previous release, have disappeared have been significantly reduced in V3.0.**

1.5 Latency

- L2C: 24 – 48-hour latency.
- L3 8-day running average: 3-day latency (after the end of the averaging period).
- L3 monthly average: 3-day latency (after the end of the averaging period).

1.6 Spatial Resolution

- 40-km product: 39 km x 47 km elliptical footprint, same as SMAP L1A antenna temperatures.
- 70-km product: circular footprint with 75 km diameter.

For most open ocean applications, the 70-km products are the best to use as they have significantly lower noise than the 40-km products.

1.7 Known Issues

1. We observe a significant degradation in retrieval performance during the early months of the SMAP mission (APR 2015 – AUG 2015). It might be related to instrument calibration, but the exact cause is currently unknown and needs further investigation. See Section 5.2 for more information.
2. The SMAP V3 land correction degrades quickly if g_{land} exceeds 1%. We recommend that V3.0 SMAP Level 2C salinities be used with care if g_{land} exceeds 1%. For the Level 3 processing, data with $g_{\text{land}} > 0.8\%$ are discarded. See Section 3.7.2 for more information.

2. LEVEL 2 PROCESSING

2.1 Input

The RSS SMAP salinity retrieval algorithm ingests RFI filtered antenna temperatures (TA) from the Version 4 SMAP L1B data files (Piepmeier et al., 2018) together with basic spacecraft ephemeris information (S/C location, velocity, and attitude) and time of observation.

2.2 Optimum Interpolation (OI) onto Fixed Earth Grid (L2A)

As a first step, we perform a Backus-Gilbert type optimum interpolation (OI) (Stogryn 1978, Poe 1990) and resample the L1B TA onto a fixed 0.25° Earth grid. The resulting gridded TAs are known as Level 2A files. The resampling is done separately for the forward (for) and the backward (aft) look. The 40-km product maintains the approximate spatial resolution and shape (39 km x 47 km) of the original SMAP L1B swath observations (Piepmeier et al., 2018). The target of the 70-km product is a circle whose diameter is about 75 km. The noise in the 70-km product is greatly reduced when compared to the 40-km product.

2.3 Ancillary Fields (L2B)

The ancillary sources for the V3.0 Level 2 processing are listed in Table 1. The ancillary fields are space-time interpolated to the location and time of the L2A data in order to create Level 2B files.

Table 1: Ancillary data sources.

Ancillary Input	Data Source
sea surface temperature	Canadian Meteorological Center. 2016 GHRST Level 4 CMC 0.2deg Global Foundation Sea Surface Temperature Analysis. Version. 3.0. doi: 10.5067/GHCMC-4FM03, http://dx.doi.org/10.5067/GHCMC-4FM03 .
sea surface wind speed and direction	CCMP V2.0 near-real time wind speed and direction. http://www.remss.com/measurements/ccmp/ . (Wentz et al. 2015.).
atmospheric profiles for pressure, height, temperature, relative humidity, cloud water mixing ratio	NCEP GDAS 1-deg 6-hour. HGT, PRS, TMP, TMP, RH, CLWMR. Available from http://nomads.ncep.noaa.gov/ .
IMERG rain rate	Huffman, G. et al., 2018. NASA Global Precipitation Measurement (GPM) Integrated Multi-Satellite Retrievals for GPM (IMERG) Version 5, LATE RUN, 30-minutes, NASA, https://pmm.nasa.gov/sites/default/files/document_files/IMERG_FinalRun_V05_release_notes-rev3.pdf .
solar flux	Noon flux values from US Air Force Radio Solar Telescope sites 1415 MHz values. Available from NOAA Space Weather Prediction Center, www.swpc.noaa.gov .
total electron content (TEC)	IGS IONEX TEC files. Available from ftp://cddis.gsfc.nasa.gov/pub/gps/products/ionex/ .
sea ice fraction	NCEP sea ice fraction. Available from http://nomads.ncep.noaa.gov/pub/data/nccf/com/omb/prod/ .

land mask	1 km land/water mask from OCEAN DISCIPLINE PROCESSING SYSTEM (ODPS). Based on World Vector Shoreline (WVS) database and World Data Bank. Courtesy of Fred Patt, Goddard Space Flight Center, frederick.s.patt@nasa.gov .
galactic map	Dinnat, E.; Le Vine, D.; Abraham, S.; Flourey, N. Map of Sky Background Brightness Temperature at L-Band. 2018. Available online at https://podaac-tools.jpl.nasa.gov/drive/files/allData/aquarius/L3/mapped/galaxy/2018 .
reference salinity (HYCOM)	Hybrid Coordinate Ocean Model, GLBa0.08/expt_90.9, Top layer salinity. Available at www.hycom.org .
Scripps ARGO salinity (only included in rain-filtered L3 monthly files)	monthly 1-degree gridded interpolated ARGO SSS field provided by Scripps. Available at www.argo.ucsd.edu/Gridded_fields.html .

2.4 Salinity Retrieval (L2C)

The SMAP salinity retrieval algorithm is then run on these Level 2B files and produces calibrated SMAP Level 2C surface ocean brightness temperatures (TB) and sea surface salinity (SSS) values.

3. SMAP SALINITY RETRIEVAL ALGORITHM

3.1 Overview and Basic Flow

The SMAP Level 2C salinity retrieval algorithm (Figure 1) has been adapted from the Aquarius Level 2 Version 5.0 (final release) salinity retrieval algorithm and configured for SMAP (Meissner et al. 2017, 2018).

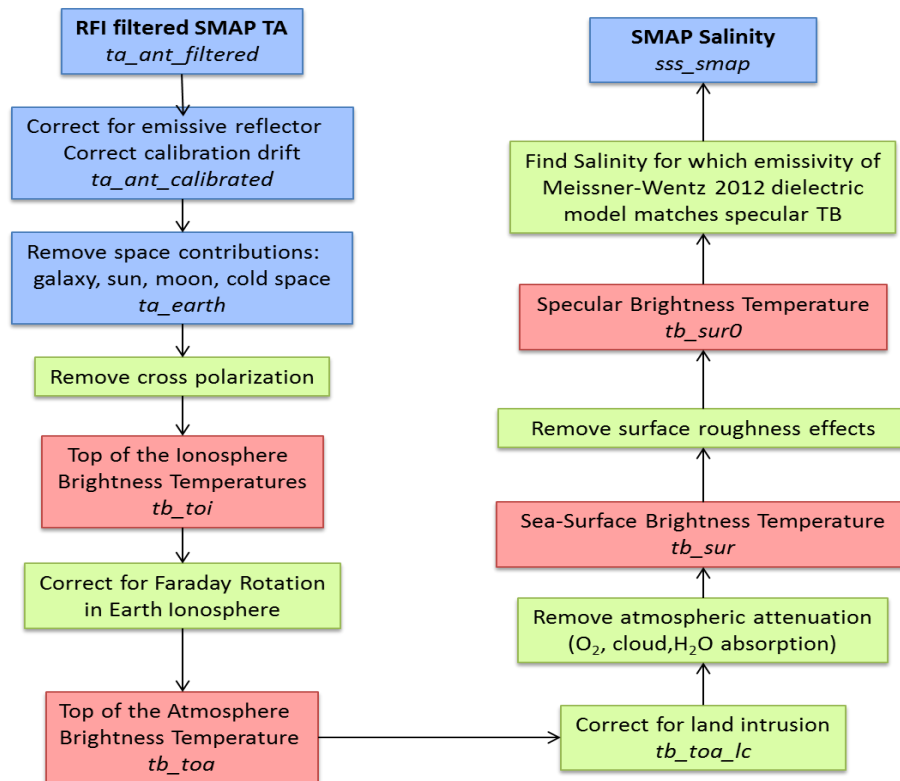


Figure 1: Flow diagram of the SMAP salinity retrieval algorithm.

We use equal channel weights of 1.0 for v-pol and h-pol in the MLE for the salinity retrieval.

3.2 Surface Roughness Correction

3.2.1 Ancillary Input for Wind Speed and Direction

Due to the loss of the SMAP radar in early July 2015, there are no scatterometer wind speeds available for performing the surface roughness correction. Because of this, the surface roughness correction required to perform the V3.0 SMAP salinity retrievals uses ancillary wind speeds and directions from the CCMP V2.0 near-real (NRT) time product (Atlas et al. 2011; Wentz et al. 2015; www.remss.com/measurements/ccmp/). This Level 4 wind vector product is produced daily at RSS using a variational assimilation (VAM) of different satellite wind products and a background wind field. The spatial gridding is $0.25^\circ \times 0.25^\circ$ and the time resolution is 6-hours (00Z, 06Z, 12Z, 18Z). The V2.0 NRT CCMP assimilates RSS wind speed and wind direction measurements from the RSS Version 7/8 ocean suite, which includes data from the following

sensors: WindSat, SSMIS F16, F17, F18, GMI and AMSR2. Because of latency, observations from RSS ASCAT and from buoys are not ingested into the V2.0 NRT CCMP processing. The background field is the 0.25° field from NCEP GDAS.

3.2.2 Wind Induced Emissivity Model

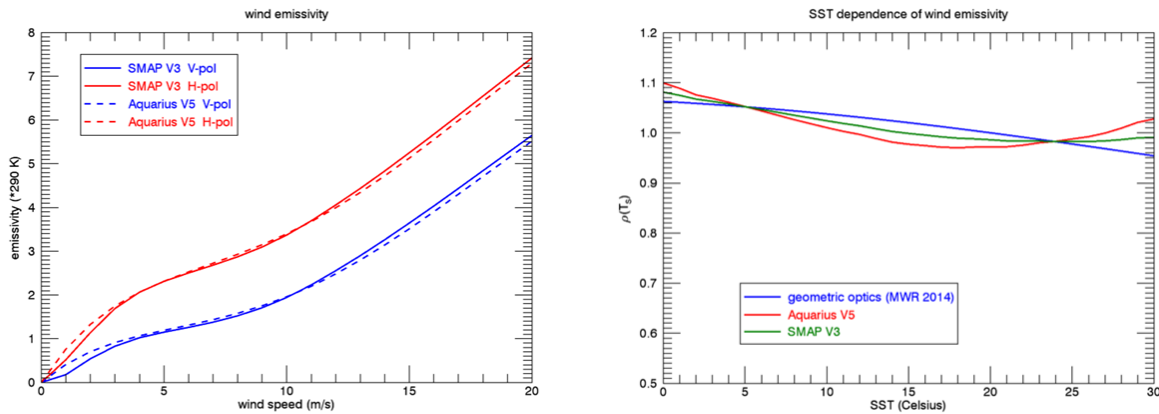


Figure 2: Left: Isotropic (wind-direction independent) part of the wind induced emissivity that is used in the Aquarius Version 5 after interpolating to the SMAP Earth Incidence Angle (dashed lines) and the SMAP Version 3 (full lines) releases. Blue: V-pol. Red: H-pol. The figure shows the 0th harmonic of the wind induced excess emissivity (Meissner et al. 2014, 2017) multiplied by 290 K. Right: SST dependence of the wind induced emissivity for Aquarius horn 2 H-pol. The blue line is the SST dependence from Meissner et al. 2014, which is predicted by the geometric optics model for the wind induced surface emission (Meissner et al. 2012). The red line is the SST dependence used in the Aquarius Version 5 release. The green line is the SST dependence used in the SMAP Version 3 release (Meissner et al. 2018).

The wind induced emissivity model for the SMAP Version 3 release is based on the wind emissivity model of the Aquarius V5 release after interpolating it to the SMAP Earth incidence angle. There is a small adjustment applied to the Aquarius V5 model function in the SMAP V3 release. This is due to the fact that the CCMP ancillary field is slightly different from the Aquarius HHH wind speed which was used in the Aquarius Version 5 algorithm. Small biases on the order of 0.1 m/s exist between these two ancillary wind fields and are dependent on wind speed as well as SST. Because of the high level of accuracy that is required for retrieving salinity, these biases need to be considered when deriving the wind induced emissivity model function for SMAP Version 3 using the method outlined in Meissner et al. 2014. As a consequence of the slightly different ancillary wind speed inputs to the Aquarius Version 5 and SMAP Version 3 salinity retrieval algorithms, the geophysical model functions for the wind emissivities also differ slightly. This is most important for the wind speed dependence 0th harmonic coefficient of the wind induced emissivity i.e., the isotropic part. This is shown in the left panel of Figure 2 for both SMAP polarizations. Small differences are observable at very low and at very high wind speeds. This coincides with the instances where small differences between Aquarius HHH and CCMP wind speeds exist. In addition, we have also found slight differences in the SST dependence $\rho(T_s)$ of the wind induced emissivity, which is shown in the right panel of Figure 2 for the h-pol. The correction term $\rho'(T_s)$ in equation (1) of Meissner et al. 2018, which is empirically

determined, is the deviation from the theoretical value predicted by the geometric optics model (Meissner and Wentz 2012; Meissner et al. 2014). This value is reduced by 50% in SMAP Version 3 when compared to Aquarius Version 5. Consequently, the value of $\rho(T_s)$ in SMAP Version 3 lies between the theoretical value of the geometrics optics model and the value of Aquarius Version 5.

The derivation of the SMAP V3 wind roughness model uses ARGO Scripps salinity as a reference field to compute the flat surface emission.

FORTRAN90 and IDL routines that compute the SMAP V3 wind induced emissivity model function are available together with these release notes at www.remss.com/missions/smap/.

3.3 Correction for Emissive SMAP Antenna

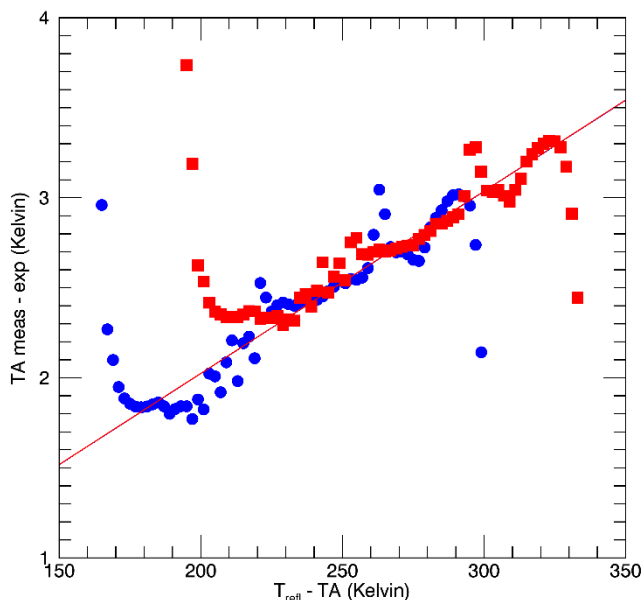


Figure 3: Regression of T_A measured minus expected versus $T_{refl} - T_A$. T_{refl} is the physical temperature of the antenna. T_A is the radiometric antenna temperature. Blue: V-pol. Red: H-pol. The slope of the linear fits is the reflector emissivity.

The emissivity of the Aquarius antenna was negligible for all practical purposes. SMAP, however, has a mesh reflector which has an emissivity of about 1%. This is large enough that a correction needs to be applied in the salinity retrieval. If T_A is the antenna temperature before the radiation hits the reflector whose physical temperature is denoted by T_{refl} and whose emissivity is ε_{refl} , then the resulting antenna temperature T_A' that enters the receiver after the reflection is given by:

$$T_A' = (1 - \varepsilon_{refl}) \cdot T_A + \varepsilon_{refl} \cdot T_{refl} = T_A + \varepsilon_{refl} \cdot (T_{refl} - T_A) \quad (1)$$

In order to perform this emissivity correction i.e., determine the value of T_A from the measured T'_A according to (1), it is necessary to know the values of both the reflector emissivity ϵ_{refl} and its physical temperature T_{refl} .

The value of the reflector emissivity ϵ_{refl} can be determined by performing a linear regression of the SMAP $\Delta T_A = T_{A,meas} - T_{A,exp}$ against $T_{refl} - T'_A$ before performing any correction for the emissive reflector. The slope of this regression is ϵ_{refl} . We have determined values of $\epsilon_{refl} = 0.01012$ for both V-pol and H-pol (Figure 3). Similar values are used in the Version 4 L1B files (Piepmeier et al. 2018). It is worth noting that these values for the reflector emissivity are about 4 times larger than the values that were determined pre-launch.

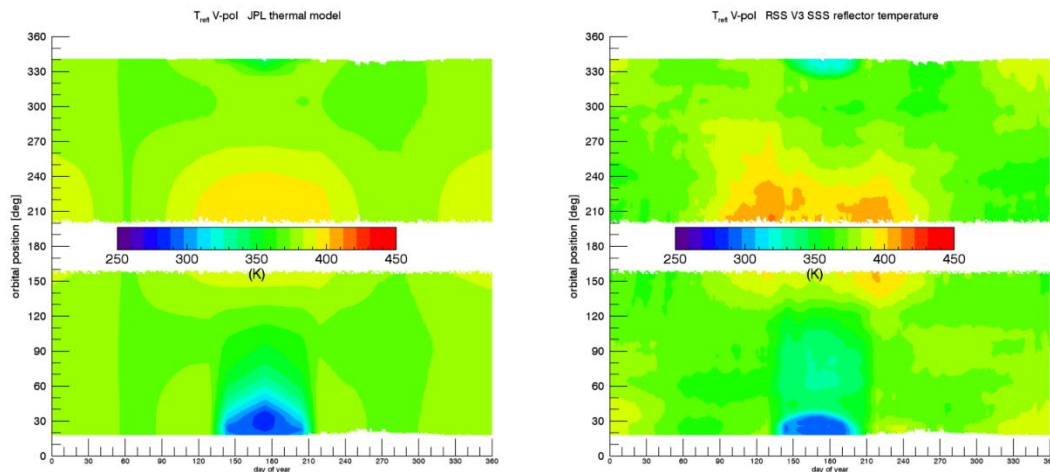


Figure 4: Physical temperature T_{refl} of the reflector. Left: JPL thermal model that is used in the SMAP L1B files (Piepmeier et al. 2018). Right: Empirical adjustment in the RSS SMAP Version 3 salinity release.

There are no direct measurements of the physical temperature T_{refl} of the SMAP mesh antenna. Instead, only a thermal model for the SMAP reflector, which was developed and run by the Jet Propulsion Laboratory (JPL) thermal modeling team, is available (Figure 4 left). The values of this JPL thermal model are used and included in the SMAP L1B files (Piepmeier et al. 2018). Our analysis has revealed that the JPL thermal model is not accurate enough to retrieve ocean salinity from SMAP without adjustments. This can be seen from the Hovmoeller diagram in Figure 5, which shows the bias of $T_{A,meas} - T_{A,exp}$ as function to time (day of year) and orbital position (z-angle) using the JPL thermal model in the emissive reflector correction. In the computation of $T_{A,exp}$ we have used Scripps ARGO as reference salinity. The zonal and temporal biases increase significantly get large when the spacecraft goes in and out of solar eclipse during the summer months and it is also large during the winter months. In those instances, rapid cooling or heating of the SMAP reflector occurs. According to our analysis, the thermal models can

overestimate or underestimate the rate of these thermal changes. The observed zonal and temporal biases in Figure 5 are largely independent of the SMAP look direction. These biases differ significantly between ascending (lower half of the diagram) and descending (upper half of the diagram) swaths because the thermal heating and cooling of the SMAP antenna is not symmetric between the two swaths. This leads us to believe that these biases are indeed caused by inaccuracies in the JPL thermal model rather than by other sources such as galaxy correction or sun intrusion, which would strongly depend on look direction. It also seems unlikely that these biases are due to errors in dielectric model or surface roughness correction since these are expected to be largely the same in the ascending and descending swaths. It was decided for the SMAP V3 salinity retrievals to make an empirical adjustment to the JPL thermal model, whose purpose is to minimize the zonal and temporal biases in $\Delta T_A = T_{A,meas} - T_{A,exp}$ when the correction for the emissive reflector is performed with this empirically adjusted model. This was done by taking the values for the ΔT_A biases from Figure 5 and computing the corresponding value of ΔT_{refl} from equation (1). The empirical ΔT_{refl} depends on time (day of the year) and orbital angle (z-angle). The same empirical correction is used for all years. The result for the empirically adjusted thermal model in the SMAP Version 3 salinity release is shown in Figure 4 (right). We use the same thermal model adjustments for V-pol and H-pol. The values for ΔT_{refl} are included in the L2C files.

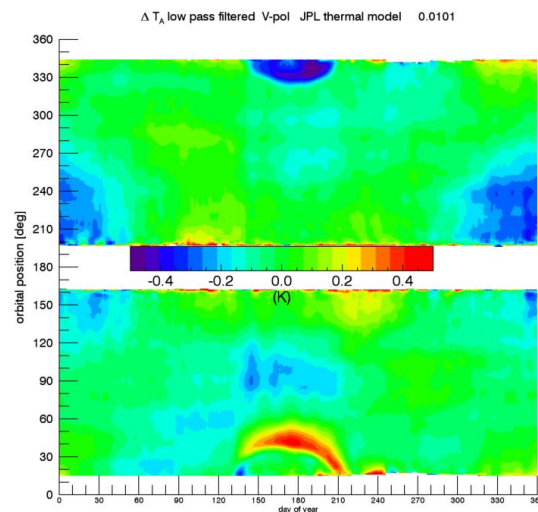


Figure 5: Hovmoeller diagram of SMAP TA measured - expected over the open ocean using the JPL thermal model for the SMAP mesh antenna. The x-axis is time (day of year) and the y-axis is orbital position (z-angle). For the computation of ΔT_A we have used Scripps ARGO as reference salinity. The computation of this diagram is based on 2 years of SMAP data (September 2015 – August 2017). A simple spatial and temporal low-pass filter was applied by performing a running average in both dimensions.

In our approach to empirically determine both ε_{refl} and T_{refl} for SMAP, we have tried to avoid folding potential errors in one quantity into the other. When determining the value of ε_{refl}

from the linear regression (Figure 3), we only used cases where the JPL thermal model was determined to be accurate i.e., where the biases in Figure 5 are small (less than 0.1 K).

3.4 Atmospheric Oxygen Absorption

The SMAP Version 2 release used the oxygen absorption model by Wentz and Meissner (2016). The SMAP Version 3 release uses the oxygen absorption model by Liebe et al. (1992), as does the Aquarius Version 5 release.

3.5 IMERG Rain Rate and Correction for Liquid Cloud Water Absorption

The SMAP Version 2 salinity retrieval algorithm uses cloud water density profiles from NCEP GDAS. Analysis has shown that these NCEP cloud water profiles are very unreliable and therefore cannot serve as a realistic source for a cloud water absorption correction in the salinity retrieval algorithm.

The IMERG rain product (Huffman et al. 2018), available from <https://pps.gsfc.nasa.gov/>, is a Level 4 merged product for surface rain rates, which is largely based on observations by NASA's Global Precipitation Mission (GPM). It is currently regarded as the best available merged rain product by the scientific community. It is available for the whole SMAP operational period. We use the 30-minute 0.1 deg product.

The IMERG rain rate R_{IMERG} is resampled from 0.1 deg to the 40/70 km SMAP resolution. We then transform the resampled IMERG rain rate into columnar liquid cloud water content L following the method by Hilburn and Wentz (2008). From L we compute the columnar absorption A_L by liquid cloud water assuming Rayleigh approximation using the dielectric constant for pure (cloud) water by Meissner and Wentz (2004). With the updated value for A_L from IMERG, we can then recompute the atmospheric parameters τ , T_{BUP} , T_{BDW} , that enter the atmospheric absorption correction (Meissner et al. 2017, 2018).

The IMERG rain rate is also used for rain flagging in the ocean-target calibration (Section 3.9) and for producing the rain-flagged monthly Level 3 data (Section 4.2).

3.6 Correction for Reflected Galaxy

The correction for the reflected galaxy uses a combination of the geometric optics model for reflection from rough ocean surfaces and the results from the SMAP for – aft look analysis. It is described in detail in Meissner et al. 2017 and Meissner et al. 2018. The empirical zonal symmetrization that was done in the Aquarius Version 5 release is **not** done for the SMAP V3 release.

3.7 Land Correction

3.7.1 Computation of the SMAP V3 Land Correction

The Aquarius SMAP salinity retrievals degrade quickly as the footprint gets within 500km of land. This land-contamination error occurs because the land is radiometrically much warmer than the ocean. When the satellite observation gets close to land, a correction for land

entering the antenna sidelobes can be derived from simulated Aquarius and SMAP brightness temperatures (Meissner et al. 2017, 2018).

The land contamination is most conveniently dealt with at the TOA (top of the atmosphere). The error due to this contamination is given as:

$$\Delta T_{B,TOA} = \hat{T}_{B,TOA} - \bar{T}_{B,TOA,ml} \quad (2)$$

The 1st term on the right hand side of equation (2) is the *observed* (i.e., measured) signal, which is computed by simulating TOA Earth brightness temperatures containing representative ocean and land scenes and integrating them over the SMAP antenna gain pattern. The 2nd term of the right hand side of equation (2) is the *true* TOA TB coming from the antenna main beam. Using the simulated SMAP TB, a table of the $\Delta T_{B,TOA}$ is computed one time off-line before the algorithm is run. In addition, the antenna gain weighted land fraction g_{land} is computed by integrating the antenna gain over the land covered area.

When computing the values for g_{land} and $\Delta T_{B,TOA}$ in the SMAP Version 2 release, it was assumed that the position of the equatorial crossing repeats itself exactly every 8 days. This assumption is not accurate because there are small shifts in the equatorial crossing position from the target position. This has resulted in inaccuracies in the salinity retrievals near the coast after the land correction is applied.

In Version 3, the computation of g_{land} and $\Delta T_{B,TOA}$ no longer operates under this assumption. Rather, we keep the equatorial crossing as a variable degree of freedom as was done in the Aquarius Version 5 land correction (Meissner et al. 2017; 2018). Because SMAP performs a full 360° scan, the sidelobe correction needs to be derived for a series of different scan positions. The g_{land} and $T_{B,TOA}$ land correction tables in SMAP Version 3 depend on:

1. Polarization (v-pol, h-pol).
2. Cell longitude (720 elements in 0.5° increment).
3. Cell latitude (361 elements in 0.5° increment).
4. Ascending/descending (2 elements).
5. Scan angle (30 elements in 12° increments).
6. The $T_{B,TOA}$ land correction tables also depend on time (12 month). The g_{land} tables do not.

These variables result in the SMAP V3.0 $T_{B,TOA}$ land correction table having a dimensionality of (2, 720, 361, 2, 30, 12), which corresponds to 374,284,800 elements. The computation of the g_{land} and $T_{B,TOA}$ land correction tables in SMAP Version 3 follows the same procedure as in Aquarius Version 5 (Meissner et al. 2017, 2018).

3.7.2 Results and Performance of Land Correction

The performance results for the V3.0 land correction are shown in Figure 6 and Figure 7. If the gain weighted land fraction g_{land} is below 1%, the V3.0 represents a clear improvement in bias and standard deviation over no land correction as well as the V2.0 land correction. However, if g_{land} gets above 1%, the V3.0 land correction becomes noisier than if no land correction is applied. We recommend that V3.0 SMAP Level 2C salinities be used with care if g_{land} exceeds 1%. For the Level 3 processing, data with $g_{land} > 0.8\%$ are discarded.

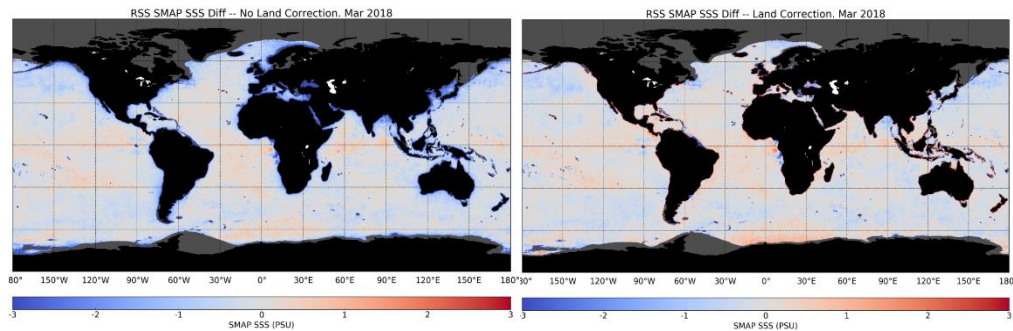


Figure 6: Monthly map of SSS SMAP – HYCOM for March 2018. Left: without land correction. Right: Using the V3.0 land correction.

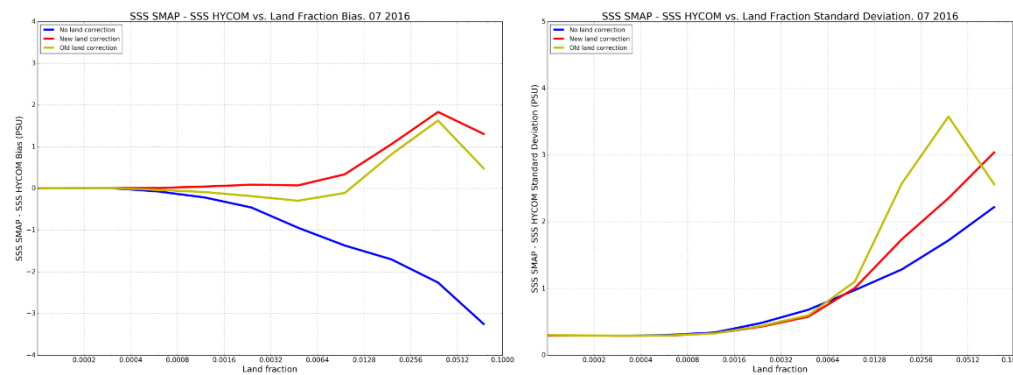


Figure 7: Bias (left) and standard deviation (right) of SMAP salinity retrievals versus HYCOM SSS for July 2017: blue = without any land correction, olive = using the V2.0 land correction, red = using the V3.0 land correction.

3.8 Antenna Pattern Correction (APC)

The A-matrix \mathbf{A} transforms Stokes vector of the Earth $\mathbf{T}_{A,Earth}$ into TOI (top of the ionosphere) \mathbf{T}_B (Meissner et al. 2017):

$$\mathbf{T}_{B,TOI} = \mathbf{A} \cdot \mathbf{T}_{A,Earth} \quad (3)$$

The SMAP 4 by 4 A-matrix elements are computed from SMAP pre-launch antenna patterns that have been created by the JPL antenna group from the GRASP software (file *SMAP_Antenna_Pattern_verF_Freq1413_Ang000_2D.dat*, provided by Emmanuel Dinnat, GSFC).

For the Version 3 release, we have adjusted some of the A-matrix elements. These adjustments were done in order to:

1. Get the best TB over ocean scenes and the Amazon rainforest for all 4 Stokes parameters (I, Q, S3, S4).
2. Minimize spurious observed cross-talk dependencies between I, Q and S3, S4.

The A-matrix elements of the V3 salinity release are listed in Table 2.

Table 2: A-matrix elements A_{ij} (in I, Q, S3, S4 basis) of the SMAP V3 release. The entries in red denote matrix elements that differ from the pre-launch computation.

	j=1	j=2	j=3	j=4
i=1	1.0929	-0.0001	0.0036	-0.0006
i=2	0.0000	1.1349	+0.0066	-0.0001
i=3	0.0009	0.0042	1.1336	-0.0553
i=4	0.0003	0.0014	+0.0117	1.1297

The non-linear IU coupling that was observed in the Aquarius data (Meissner et al. 2017) is not observed with SMAP.

3.9 Ocean Target Calibration

The ocean target calibration (Meissner et al. 2017, 2018) removes any remaining, constant and time-varying biases in the TA measured – expected over the open ocean. We calculate the 3-day running average of TA measured – expected $\langle \Delta T_A(i) \rangle = \langle T_{A,meas}(i) - T_{A,exp}(i) \rangle$ as well as the average $\langle T_A(i) \rangle$ for each orbit i over the open ocean for rain free scenes. The computation of TA expected uses HYCOM as reference salinity. We require that the land fraction g_{land} and the sea-ice fraction g_{ice} are both less than 0.0005, the IMERG rain rate is less than 0.1 mm/h (bit 15 in Table 3) and the flags for sun-glint (bit 5 in Table 3), moon-glint (bit 6 in Table 3) and high reflected galaxy (bit 7 in Table 3) are not set.

The values of $\langle \Delta T_A(i) \rangle$ and $\langle T_A(i) \rangle$ are included in the metadata of the L2 files. We assume that any remaining calibration adjustment is an effective adjustment of the noise-diode temperature T_{ND} . If T_{Ap} is the antenna temperature of a SMAP observation for polarization $p = V$ or H after correcting for the emissive reflector, then we calculate the *calibrated antenna temperature* $T_{A,cal}$ as:

$$T_{Ap,cal} = T_{Ap} - \frac{\langle \Delta T_{A,p}(i) \rangle}{\langle T_{Ap}(i) \rangle - \langle T_D \rangle} \cdot (T_{Ap} - \langle T_D \rangle) \quad p = V, H \quad (4)$$

The $\langle T_D \rangle$ in equation (4) stands for an average value of the Dicke load temperature. For our purposes, we set this to a value of 293 K. Per construction, the running 3-day average of $T_{Ap,cal}$ is zero for each orbit: $\langle T_{Ap,cal}(i) \rangle = 0$.

We have also found small offsets for the S3 and S4, which are constant in time after the SMAP radar was shut off but differ during time period before that. The following offset correction for S3 and S4 is performed:

$$T_{Ap,cal} = T_{A,p} - \langle T_{A,p,offset} \rangle \quad p = S3, S4 \quad (5)$$

The offset values $\langle T_{A,p,offset} \rangle$ are +0.22 K (for S3) and -0.43 K (for S4) for the time after orbit # 2812. For the time before orbit # 2812, the offset values are 0.43 K (for S3) and -0.17 K (for S4).

3.10 Quality Control (Q/C) Flag

The V3.0 salinity retrieval algorithm produces the following Q/C flags:

Table 3: 32-bit Level 2 Q/C flags in the SMAP V3.0 release.

bit	Q/C flag if bit is set	SSS value and expected level of degradation
0	no valid radiometer observation in cell	SSS value set to missing/invalid
1	problem with OI: parameter <i>wt_sum</i> not normalized to 1	SSS value set to missing/invalid
2	strong land contamination: gain weighted land fraction <i>gland</i> exceeds 0.1	SSS value set to missing/invalid
3	strong sea ice contamination: gain weighted land fraction <i>gice</i> exceeds 0.1	SSS value set to missing/invalid
4	MLE in SSS retrieval algo has not converged: <i>iflag_sss_conv</i> = 1	SSS value set to missing/invalid
5	sunlint: sunlint angle <i>sunslt</i> between 0° and 50° and scan angle <i>alpha</i> between 30° and 150°	SSS retrieved very strong degradation
6	moonglint: moonglint angle <i>monglt</i> less than 15°	SSS retrieved moderate – strong degradation
7	high reflected galaxy: 1 st component <i>ta_gal_ref</i> (1, ...)/2 [(V+H)/2] exceeds 2.0K.	SSS retrieved moderate – strong degradation
8	moderate land contamination: gain weighted land fraction <i>gland</i> exceeds 0.01	SSS retrieved moderate -strong degradation
9	sea ice contamination: gain weighted sea ice fraction <i>gice</i> exceeds 0.001	SSS retrieved moderate – strong degradation
10	high residual of MLE in SSS retrieval algo: Variable <i>tb_consistency</i> exceeds 1.0 K.	SSS retrieved moderate – strong degradation
11	low SST: <i>surtep</i> - 273.15 below 5°C	SSS retrieved moderate – strong degradation
12	high wind speed: <i>winspd</i> exceeds 15 m/s	SSS retrieved moderate degradation
13	light land contamination gain weighted land fraction <i>gland</i> exceeds 0.001	SSS retrieved light degradation
14	light sea-ice contamination gain weighted land fraction <i>gice</i> exceeds 0.0005	SSS retrieved light degradation
15	rain flag: IMERG rain-rate (resampled to SMAP footprint) exceeds 0.1 mm/h.	SSS retrieved possible light degradation due to degraded wind speed or poor atmospheric correction. Validation of SMAP versus ARGO/HYCOM might result in error due to SSS stratification within the upper ocean layer
16 - 31	sparse	

4. LEVEL 3 PROCESSING

4.1 Standard Product

Both the 40km and 70km L2C salinity values are gridded into the Level 3 data product. The L3 grids are regular 0.25° latitude/longitude Earth grids created by averaging all valid L2C observations within each grid cell. For and aft looks are averaged together. We produce a running 8-day average L3 and a monthly average L3 file. For an 8-day running average that is centered on a given day *DOY* we use observations within +/- 3.5 days of *DOY*. For example, the L3 file for January 15 is created by averaging L2 observations that fall between 12UTC January 11 and 12 UTC January 19. The reason for providing 8-day averages rather than weekly averages is that SMAP has an exact 8-day repeat cycle.

During the gridding for both the 8-day running averages and the monthly averages we apply Q/C checks and discard data if:

1. The sun glint angle is less than 50° and the azimuthal look angle lies between 30° and 50° (bit 5 in L2 Q/C flag Table 3 is set).
2. The moon glint angle is less than 15° (bit 6 in L2 Q/C flag Table 3 is set).
3. The v/h-pol average of the reflected galactic radiation exceeds 2.0 K (bit 7 in L2 Q/C flag Table 3 is set).
4. The TB consistency, which is defined as the $\sqrt{\chi^2}$ of the MLE in the salinity retrieval algorithm, exceeds 1.0 K (bit 10 in L2 Q/C flag Table 3 is set).
5. The gain weighted land fraction g_{land} exceeds 0.008 (see Section 3.7.2).
6. The gain weighted sea ice fraction g_{ice} exceeds 0.001.
7. The wind speed exceeds 20 m/s.

The L3 files contain the number of observations in each grid cell as well as averaged values of salinity, g_{land} , g_{ice} , and the ancillary SST in each grid cell.

Browsing images for both 8-day and monthly averages at 40km and 70km resolution are available at the RSS website

4.2 Rain Filtered (RF) Product

In Version 3 we also produce a rain-filtered (RF) monthly L3 product for both the 40km and 70km resolutions. In doing so, we discard data if the IMERG rain rate (Section 3.5), resampled to the SMAP resolution, exceeds 0.1 mm/h (bit 15 in Table 3 is set). This RF product also includes the Scripps ARGO analyzed salinity field to allow easy comparison with the SMAP retrievals. Because of the latency of the Scripps ARGO field (a couple months), the latency of the L3 RF monthly product is larger than that of the standard monthly L3 product. The RF monthly product is only distributed at the RSS website and is not available from PO.DAAC.

5. PERFORMANCE ESTIMATE AND VALIDATION

5.1 Spatial Resolution and Noise Figures

When comparing SMAP SSS with the HYCOM SSS field, we find that the SMAP Level 2C SSS at 40km resolution have an estimated accuracy of about 0.9 psu due to the high noise figures of the L1B TA, which is input into the L2 processing.

When comparing the SMAP Level 2C SSS at a 70km resolution to the HYCOM SSS field, we conclude that this product has an estimated accuracy of about 0.5 psu due to the reduction in noise caused by the spatial smoothing of the L1B TA.

5.2 Time Series of SMAP – ARGO – HYCOM Comparisons

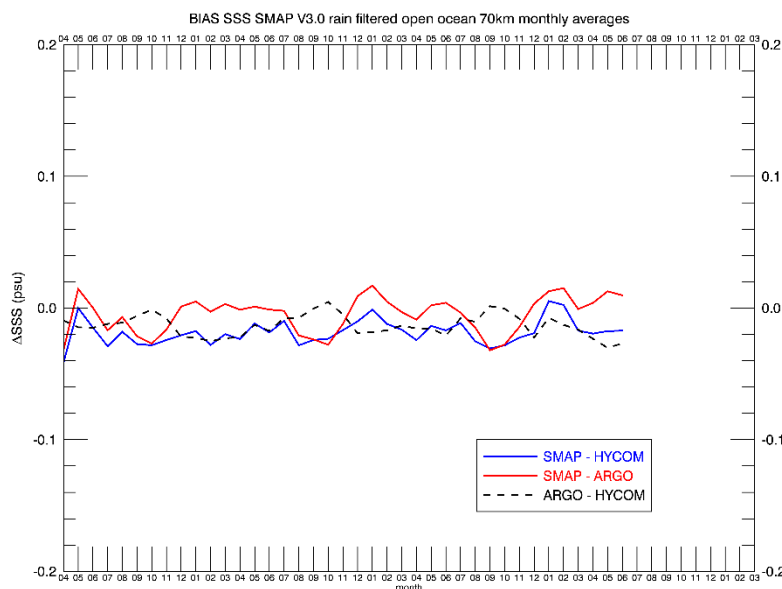


Figure 8: Time series (APR 2015 – JUN 2018) of biases: SMAP V3 – HYCOM (blue). SMAP V3 – Scripps ARGO (red). Scripps ARGO – HYCOM (dashed black). The figure was created from the Level 3 70km rain-filtered monthly maps requiring $g_{land} < 0.001$, $g_{ice} < 0.001$, $SST > 5^{\circ}C$.

Time series of biases and standard deviations between SMAP V3, Scripps ARGO and HYCOM for monthly rain-filtered averages are shown in Figure 8 - Figure 11. Assuming that the errors in the 3 data sets are uncorrelated, the RMS in the SMAP product can be estimated from the triple collocation method:

$$\sigma_{SMAP}^2 = \frac{1}{2} \cdot (\sigma_{SMAP-HYCOM}^2 + \sigma_{SMAP-ARGO}^2 - \sigma_{ARGO-HYCOM}^2) \quad (6)$$

This RMS is represented by the green curves in Figure 9 - Figure 11.

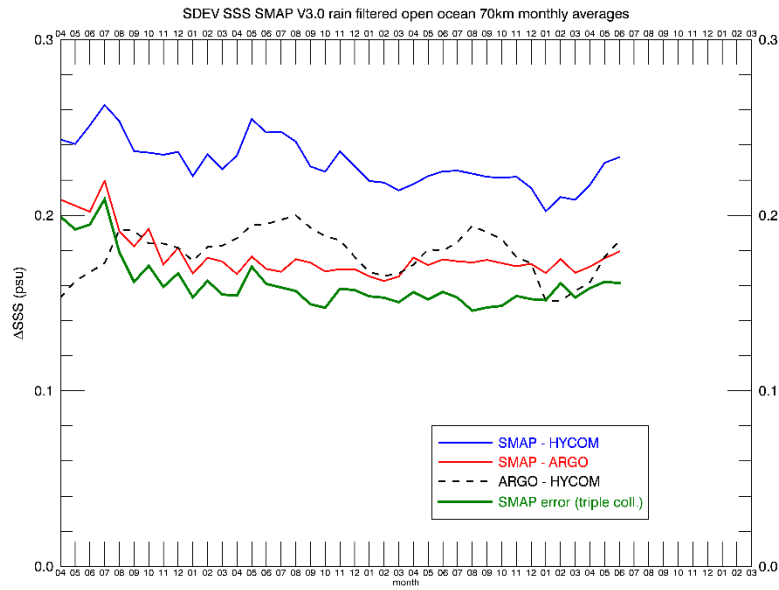


Figure 9: Time series (APR 2015 – JUN 2018) of standard deviations: SMAP V3 – HYCOM (blue). SMAP V3 – Scripps ARGO (red). Scripps ARGO – HYCOM (dashed black). The figure was created from the Level 3 70-km rain-filtered monthly maps requiring gland < 0.001, gice<0.001, SST>5°C. The green curve is the estimated RMS error in the SMAP data based on the triple collocation method.

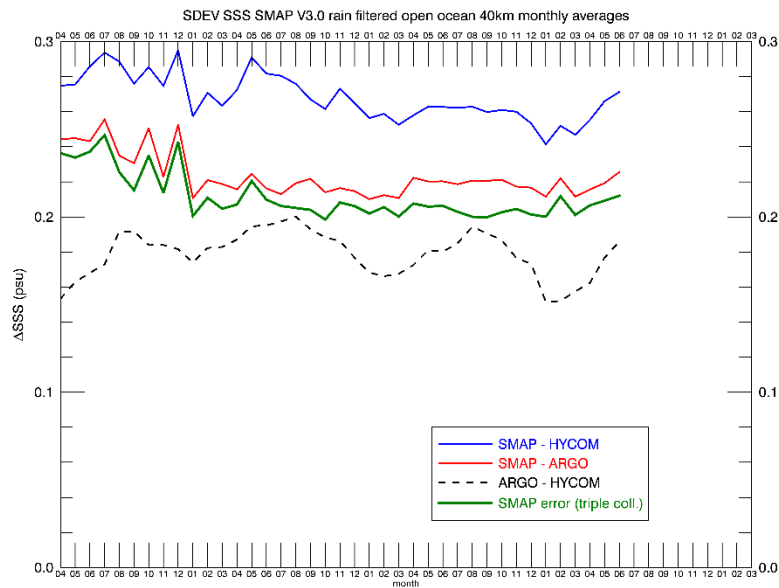


Figure 10: Same as Figure 9 for the 40-km product.

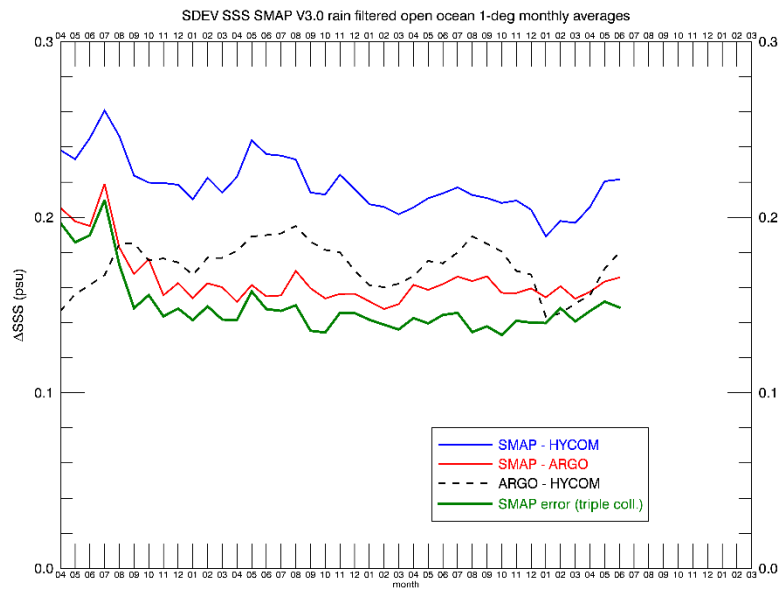


Figure 11: Same as Figure 9 for 1-deg lat/lon averages.

The noise reduction of the 70km product compared to the 40km product is still visible in the 8-day and monthly averages (Figure 9 and Figure 10).

The estimated SMAP RMS errors for the 1-deg monthly averages (Figure 11) are 0.14 – 0.15 psu (after AUG 2015). These are comparable with the Aquarius Version 5 RMS errors (Kao et al. 2018).

We observe a significant degradation in the performance during the early months of the SMAP mission (APR 2015 – AUG 2015). This might be related to instrument calibration, but its cause is currently unknown and needs further investigation.

5.3 Zonal and Average Regional Biases

Figure 12 shows a Hovmoeller diagram and Figure 13 shows a global bias map of SMAP – Scripps ARGO SSS based on the rain-filtered V3 SMAP product.

The V2 SMAP release had significant salty biases at low latitudes and fresh biases at high latitudes in the SMAP SSS. These biases have been greatly reduced in the V3 release.

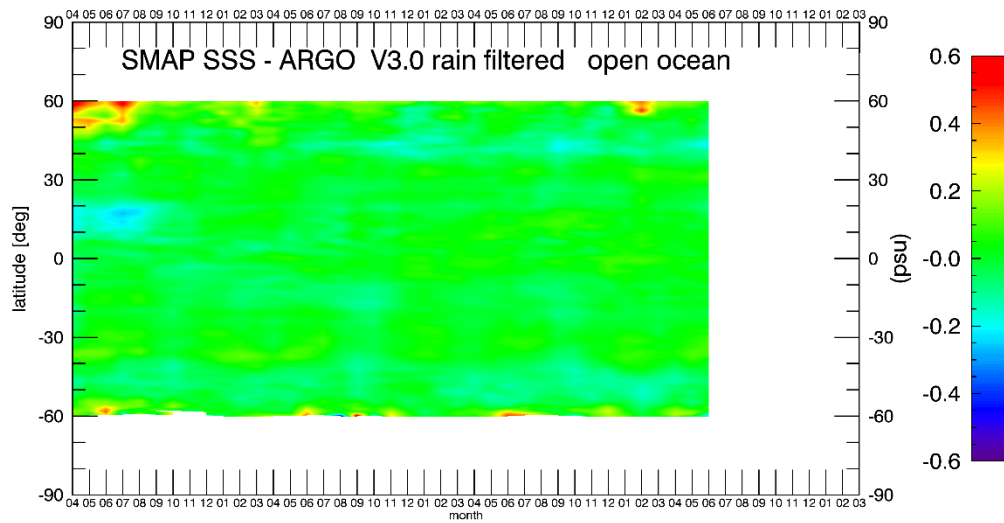


Figure 12: Hovmoeller diagram (APR 2015 – JUN 2018) of SMAP V3 SMAP V3 – Scripps ARGO. The figure was created from the Level 3 70km rain-filtered monthly maps requiring $g_{land} < 0.001$, $g_{ice} < 0.001$, $SST > 5^{\circ}C$.

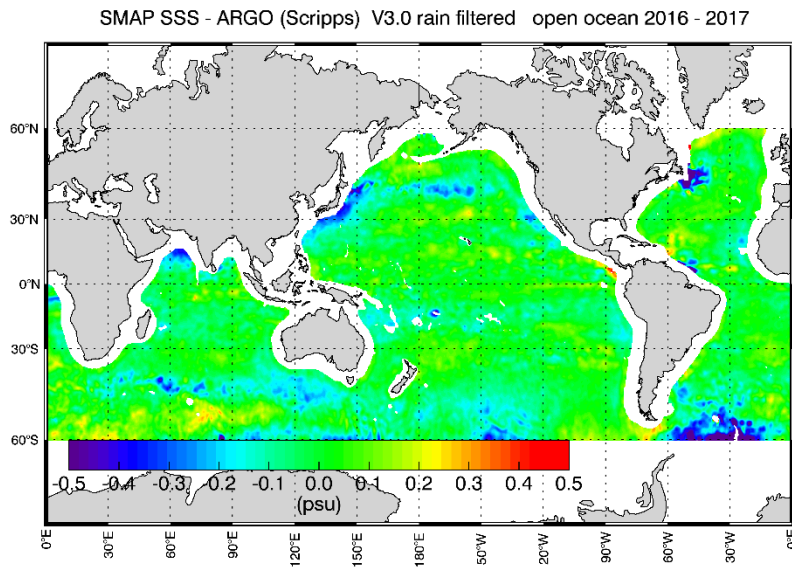


Figure 13: Global map (JAN 2016 – DEC 2017) of SMAP V3 SMAP V3 – Scripps ARGO. The figure was created from the Level 3 70km rain-filtered monthly maps requiring $g_{land} < 0.001$, $g_{ice} < 0.001$, $SST > 5^{\circ}C$.

6. REFERENCES

- Atlas, R., R. N. Hoffman, J. Ardizzone, S. M. Leidner, J. C. Jusem, D. K. Smith, D. Gombos, 2011: A cross-calibrated, multiplatform ocean surface wind velocity product for meteorological and oceanographic applications. *Bull. Amer. Meteor. Soc.*, 92, 157-174. doi: 10.1175/2010BAMS2946.1
- Hilburn, K. and F. Wentz, 2008, Intercalibrated passive microwave rain products from the unified microwave ocean retrieval algorithm (UMORA), *Journal of Applied Meteorology and Climatology*, 47, 778-794.
- Huffman, G. et al., 2018, NASA Global Precipitation Measurement (GPM) Integrated Multi-satellite Retrievals for GPM (IMERG), Version 5.2, NASA, Available online at https://pmm.nasa.gov/sites/default/files/document_files/IMERG_ATBD_V5.2_0.pdf.
- Kao, H.-Y., G. Lagerloef, T. Lee, O. Melnichenko, T. Meissner and P. Hacker, 2018, Assessment of Aquarius Sea Surface Salinity, *Remote Sens.* 10(9), <https://doi.org/10.3390/rs10091341>.
- Liebe, H., P. Rosenkranz and G. Hufford, 1992, Atmospheric 60-GHz oxygen spectrum: New laboratory measurements and line parameters, *J. Quant. Spectrosc. Radiat. Transfer*, 48, 629–643, doi: 10.1016/0022-4073(92)90127-P.
- Meissner, T. and F. Wentz, 2012, The emissivity of the ocean surface between 6 and 90 GHz over a large range of wind speeds and Earth incidence angles, *IEEE TGRS*, 2012, 50(8), 3004–3026, doi: 10.1109/TGRS.2011.2179662.
- Meissner, T., and F. Wentz, The complex dielectric constant of pure and sea water from micro-wave satellite observations, *IEEE TGRS*, vol. 42(9), pp 1836, 2004.
- Meissner, T., F. Wentz, and L. Ricciardulli, 2014: The emission and scattering of L-band microwave radiation from rough ocean surfaces and wind speed measurements from Aquarius, *J. Geophys. Res. Oceans*, vol. 119, doi: 10.1002/2014JC009837.
- Meissner, T., F. Wentz F. and D. M. Le Vine, 2017, Aquarius Salinity Retrieval Algorithm Theoretical Basis Document (ATBD), End of Mission Version; RSS Technical Report 120117; 1 December 1 2017. Available online at ftp://po-daac-ftp.jpl.nasa.gov/allData/aquarius/docs/v5/AQ-014-PS-0017_Aquarius_ATBD-EndOfMission.pdf.
- Meissner, T, F.J. Wentz, and D.M. Le Vine, 2018, The Salinity Retrieval Algorithms for the NASA Aquarius Version 5 and SMAP Version 3 Releases, *Remote Sensing* 10, 1121, doi:10.3390/rs10071121.
- Piepmeyer, J. et al., 2014: SMAP Calibrated, Time-Ordered Brightness Temperatures L1B_TB Data Product, Algorithm Theoretical Basis Document (ATBD), <https://smap.jpl.nasa.gov/documents/>.
- Piepmeyer, J. et al. 2018: SMAP L1B Radiometer Half-Orbit Time-Ordered Brightness Temperatures, Version 4. [RFI filtered antenna temperatures]. Boulder, Colorado USA. NASA National Snow and Ice Data Center Distributed Active Archive Center. <https://doi.org/10.5067/VA6W2M0JTK2N>.
- Poe, G., 1990, Optimum interpolation of imaging microwave radiometer data, *IEEE Trans. Geosci. Remote Sens.*, vol. 28, no. 5, pp. 800-810.
- Stogryn, A., 1978, Estimates of brightness temperatures from scanning radiometer data, *IEEE Trans. Antennas Propag.* vol. AP-26, no. 5, pp. 720 – 726.
- Wentz, F.J., J. Scott, R. Hoffman, M. Leidner, R. Atlas, J. Ardizzone, 2015: Remote Sensing Systems Cross-Calibrated Multi-Platform (CCMP) 6-hourly ocean vector wind analysis product on 0.25 deg grid, Version 2.0. Remote Sensing Systems, Santa Rosa, CA. Available online at www.remss.com/measurements/ccmp.
- Wentz, F., and T. Meissner, 2016: Atmospheric absorption model for dry air and water vapor at microwave frequencies below 100GHz derived from spaceborne radiometer observations, *Radio Science*, vol. 51, doi:10.1002/2015RS005858.

7. DATA FORMAT SPECIFICATION

7.1 Level 2C

7.1.1 Paths and Filenames

- **Pathname:** */smap/SSS/V03.0/FINAL/L2C/xxkm/yyyy/mm/...*
xx = 40 or 70, yyyy = 4-digit year, mm = 2-digit month.
- **Filename:** *RSS_SMAP_SSS_L2C_xxkm_rnnnnn_yyyymmddThhmiss_yyyyddd_FNL_V03.0.nc.*
xx = 40 or 70, nnnnn = 5-digit orbit (rev) #, yyyy = 4-digit year, mm = 2-digit month, dd = 2-digit day of month, hh=2-digit hour of day (UTC), mi = 2-digit minute of hour (UTC), ss = 2-digit second of minute (UTC), doy 3-digit day of year. The time stamp refers to the start time of the orbit.

7.1.2 Global Attributes

- **start_time_sec2000** (8-byte real): seconds of first valid record in this rev since 2000-01-01 00:00:00 UTC.
- **start_time_year, start_time_month, start_time_day_of_month, start_time_day_year** (4-byte integer): year, month, day of month, day of year of first valid record in this rev.
- **start_time_sec_of_day** (8-byte real): seconds of day of first valid record in this rev.
- **emissivity_reflector_vpol, emissivity_reflector_hpol** (4-byte real): ϵ_{ant} (Section 3.3).
- **A_ij** (4-byte real): APC matrix element (i, j) where the indices i, j run over the Stokes vector I, Q, S3, S4 (Section 3.8).
- **ta_ocean_ave_vpol, ta_ocean_ave_hpol** (4-byte real): average ta over open ocean for this rev (Section 3.9).
- **ta_bias_ocean_vpol, ta_bias_ocean_hpol, ta_bias_ocean_S3, ta_bias_ocean_S4** (4-byte real): TA biases= TA measured – expected over the open ocean (Section 3.9). The computation of TA expected is based on the HYCOM reference SSS. The computation of TA expected for the 3rd Stokes parameter (S3) is based on ancillary TEC maps from IGS (Table 1).

7.1.3 Gridding and Dimensions

The L2C files contain SMAP observations that were optimum interpolated onto a fixed 0.25° x 0.25° Earth grid.

The grid (x, y) dimensions are:

- **xdim_grid=1560**, which corresponds to 360° longitude plus 30° in order to accommodate the whole swath.
- **ydim_grid =720**, which corresponds to 180° latitude.

Though the grid cell indices are related to longitude and latitude, the variables cellon and cellat (Section 7.1.4) should be used to identify the location.

- **look** = 2 (1 = for look, 2= aft look) defines the look direction of the variable. If the variable does not depend on look direction, then this dimension is omitted.
- **polarization_2** = 2, **polarization_3** = 3, **polarization_4** = 4 specifies the polarization of the variable fields. Note that for some variables the Stokes polarization basis (I, Q, S3, S4) is used, whereas for other variables the modified Stokes polarization basis (V, H, S3, S4) is used. See Section 7.1.4.

Any grid cell for with one of the bits 0 – 1 set has invalid entries and none of the variable fields should be used. Any grid cells with one of the bits 2 – 3 set has no valid salinity retrieval.

7.1.4 Variables

All variable values refer to the average of the OI in the grid cell.

- **time** (8-byte float, array size = [look, xdim_grid, ydim_grid]): seconds of observation since 2000-01-01 00:00:00 UTC.
- **cellat** (4-byte float, array size = [look, xdim_grid, ydim_grid]): geodetic latitude. range: [90°S, 90°N].
- **cellon** (4-byte float, array size = [look, xdim_grid, ydim_grid]): longitude. range: [0°, 360°].
- **eia** (4-byte float, array size = [look, xdim_grid, ydim_grid]): boresight Earth incidence angle. range: [0°, 90°].
- **eea** (4-byte float, array size = [look, xdim_grid, ydim_grid]): boresight Earth azimuth angle. range: [0°, 360°].
- **zang** (4-byte float, array size = [look, xdim_grid, ydim_grid]): orbital position angle of S/C. range: [0°, 360°]. It is defined as:
$$zang = \arctan \frac{(\hat{R}_{S/C} \cdot \hat{z})}{(\hat{V}_{S/C} \cdot \hat{z})} + 90^\circ$$
. \hat{z} is the z-unit vector in the Earth centered inertial system (ECI). $\hat{R}_{S/C}$ is the S/C location unit vector in the ECI system. $\hat{V}_{S/C}$ is the S/C velocity unit vector in the ECI system. 0° is S, 90° is equator crossing in the ascending swath, 180° is N, 270° is equator crossing in the descending swath, 360° is S.
- **alpha** (4-byte float, array size = [look, xdim_grid, ydim_grid]): scan angle. range: [0°, 360°]. 0° is forward, 90° is left of forward, 180° is aft, 270° is right of forward, 360° is forward.
- **pra** (4-byte float, array size = [look, xdim_grid, ydim_grid]): polarization basis rotation angle (geometrical part), which is the angle between polarization basis of S/C and polarization basis on the Earth. range: [-90°, +90°].
- **sunglt** (4-byte float, array size = [look, xdim_grid, ydim_grid]): sun glint angle. range: [-180°, +180°]. It is the angle between specular reflection of boresight and the ray to the sun. A negative value means that the ray to the sun is piercing the Earth.
- **monglt** (4-byte float, array size = [look, xdim_grid, ydim_grid]): moon glint angle. range: [-180°, +180°]. It is the angle between specular reflection of boresight and the ray to the moon.
- **gallat** (4-byte float, array size = [look, xdim_grid, ydim_grid]): polar angle of specular reflection ray from boresight in ECI J2000 system (Earth centered inertial system of year 2000). range: [-90°, +90°].
- **gallon** (4-byte float, array size = [look, xdim_grid, ydim_grid]): azimuthal angle of specular reflection ray from boresight in ECI J2000 system (Earth centered inertial system of year 2000). range: [0°, +360°].
- **sun_beta** (4-byte float, array size = [look, xdim_grid, ydim_grid]): sun zenith angle in S/C coordinate system. [0°, +180°].
- **sun_alpha** (4-byte float, array size = [look, xdim_grid, ydim_grid]): sun azimuth angle in S/C coordinate system. [0°, +360°].
- **gland** (4-byte float, array size = [look, xdim_grid, ydim_grid]): land fraction within footprint weighted by antenna gain pattern. range: [0.0, 1.0].
- **gice** (4-byte float, array size = [xdim_grid, ydim_grid]): sea ice fraction within footprint weighted by antenna gain pattern. range: [0.0, 1.0].
- **surtep** (4-byte float, array size = [xdim_grid, ydim_grid]): ancillary sea surface temperature from CMC. units: Kelvin.
- **winspd** (4-byte float, array size = [xdim_grid, ydim_grid]): ancillary sea surface wind speed from CCMP. see Section 3.2.1. units: m/s.

- **windir** (4-byte float, array size = [xdim_grid, ydim_grid]): ancillary wind direction relative to N from CCMP. see section 3.2.1. meteorological convention. 0°: wind coming out of N, +90°: wind coming out of E, etc. range: [0°, +360°].
- **tran** (4-byte float, array size = [xdim_grid, ydim_grid]): total atmospheric transmittance. computed from ancillary NCEP GDAS atmospheric profile fields for pressure, geopotential height, temperature, relative humidity, cloud water mixing ratio. range: [0.0, 1.0].
- **tbup** (4-byte float, array size = [xdim_grid, ydim_grid]): atmospheric upwelling brightness temperature. computed from ancillary NCEP GDAS atmospheric profile fields for pressure, geopotential height, temperature, relative humidity, cloud water mixing ratio. units: Kelvin.
- **tbdw** (4-byte float, array size = [xdim_grid, ydim_grid]): atmospheric downwelling brightness temperature. computed from ancillary NCEP GDAS atmospheric profile fields for pressure, geopotential height, temperature, relative humidity, cloud water mixing ratio. units: Kelvin
- **rain** (4-byte float, array size = [xdim_grid, ydim_grid]): IMERG rain rate resampled to SMAP spatial resolution (40/70 km). see Section 3.5. units: mm/h.
- **solar_flux** (4-byte float, array size = [xdim_grid, ydim_grid]): ancillary mean solar flux from NOAA SWPC. units: SFU.
- **ta_ant_filtered** (4-byte float, array size = [polarization_4, look, xdim_grid, ydim_grid]): SMAP RFI filtered antenna temperatures. This is the basic input from the SMAP L1B TB files. units: Kelvin. polarization basis: 1=V, 2=H, 3=S3, 4=S4.
- **ta_ant_calibrated** (4-byte float, array size = [polarization_4, look, xdim_grid, ydim_grid]): SMAP antenna temperatures after correcting for the emissive antenna (Section 3.3) and after applying the ocean-target calibration (Section 3.9). units: Kelvin. polarization basis: 1=V, 2=H, 3=S3, 4=S4.
- **ta_earth** (4-byte float, array size = [polarization_4, look, xdim_grid, ydim_grid]): SMAP antenna temperatures after correcting for celestial intrusions: cold space (spillover), galaxy (direct and reflected), sun (direct and reflected), moon (reflected). units: Kelvin. polarization basis: 1=V, 2=H, 3=S3, 4=S4.
- **tb_toi** (4-byte float, array size = [polarization_4, look, xdim_grid, ydim_grid]): SMAP top of the ionosphere brightness temperatures. units: Kelvin. polarization basis: 1=V, 2=H, 3=S3, 4=S4.
- **tb_toa** (4-byte float, array size = [polarization_4, look, xdim_grid, ydim_grid]): SMAP top of the atmosphere brightness temperatures (before applying land correction). units: Kelvin. polarization basis: 1=V, 2=H, 3=S3, 4=S4.
- **tb_toa_lc** (4-byte float, array size = [polarization_4, look, xdim_grid, ydim_grid]): SMAP top of the atmosphere brightness temperatures after applying land correction (section 3.7). . units: Kelvin. polarization basis: 1=V, 2=H, 3=S3, 4=S4.
- **tb_sur** (4-byte float, array size = [polarization_4, look, xdim_grid, ydim_grid]): SMAP brightness temperature at rough ocean surface (before applying surface roughness correction, section 3.2). units: Kelvin. polarization basis: 1=V, 2=H, 3=S3, 4=S4.
- **tb_sur0** (4-byte float, array size = [polarization_4, look, xdim_grid, ydim_grid]): SMAP brightness temperature referenced to flat ocean surface (after applying surface roughness correction, section 3.2). units: Kelvin. polarization basis: 1=V, 2=H, 3=S3, 4=S4.
- **temp_ant** (4-byte float, array size = [polarization_2, look, xdim_grid, ydim_grid]): physical temperature of the SMAP mesh antenna from JPL thermal model $T_{phys,ant}$ (section 3.3). This value is included in SMAP L1B TB files. units: Kelvin. polarization basis: 1=V, 2=H.

- **dtemp_ant** (4-byte float, array size = [polarization_2, look, xdim_grid, ydim_grid]): empirical correction $\Delta T_{phys,ant}$ to the physical temperature of the SMAP mesh antenna (section 3.3). units: Kelvin. polarization basis: 1=V, 2=H.
- **ta_sun_dir** (4-byte float, array size = [polarization_3, look, xdim_grid, ydim_grid]): TA of direct sun intrusion. units: Kelvin. polarization basis: 1=I, 2=Q, 3=S3.
- **ta_sun_ref** (4-byte float, array size = [polarization_3, look, xdim_grid, ydim_grid]): TA of reflected sun intrusion. units: Kelvin. polarization basis: 1=I, 2=Q, 3=S3.
- **ta_gal_dir** (4-byte float, array size = [polarization_3, look, xdim_grid, ydim_grid]): TA of direct galaxy intrusion. units: Kelvin. polarization basis: 1=I, 2=Q, 3=S3.
- **ta_gal_ref** (4-byte float, array size = [polarization_3, look, xdim_grid, ydim_grid]): TA of reflected galaxy intrusion. units: Kelvin. polarization basis: 1=I, 2=Q, 3=S3.
- **sss_smmap** (4-byte float, array size = [look, xdim_grid, ydim_grid]): retrieved SMAP sea surface salinity. units: PSU.
- **tb_consistency** (4-byte float, array size = [look, xdim_grid, ydim_grid]):
$$\sqrt{\chi^2} = \sqrt{[T_{B,sur0} - T_{B,RTM}(SSS_{SMAP})]_{V-pol}^2 + [T_{B,sur0} - T_{B,RTM}(SSS_{SMAP})]_{H-pol}^2}$$
 of MLE in salinity retrieval algorithm. units: Kelvin.
- **iqc_flag** (4-byte integer, array size = [look, xdim_grid, ydim_grid]): 32-bit quality control flag (section 3.10).
- **sss_ref** (4-byte float, array size = [xdim_grid, ydim_grid]): ancillary reference sea surface salinity from HYCOM. units: PSU.
- **ta_ant_exp** (4-byte float, array size = [polarization_4, look, xdim_grid, ydim_grid]): expected antenna temperature before any losses. This value is to be compared with **ta_ant_calibrated**. The RTM computation is performed at boresight and based on the HYCOM reference salinity. units: Kelvin. polarization basis: 1=V, 2=H, 3=S3, 4=S4.
- **tb_sur0_exp** (4-byte float, array size = [polarization_4, look, xdim_grid, ydim_grid]): expected flat surface brightness temperature. This value is to be compared with **tb_sur0**. The RTM computation is performed at boresight and based on the HYCOM reference salinity. units: Kelvin. polarization basis: 1=V, 2=H, 3=S3, 4=S4.
- **pratot_exp** (4-byte float, array size = [look, xdim_grid, ydim_grid]): expected total polarization rotation angle = geometric part + Faraday rotation. The computation of the Faraday rotation part is based on the ancillary TEC fields from IGS. range: [-90°, +90°].

7.2 Level 3

7.2.1 Paths and Filenames

1. 8-day running averages

- **Pathname:** /smap/SSS/V03.0/FINAL/L3/8day_running/xxkm/yyyy/
- **Filename:** RSS_smmap_SSS_L3_8day_running_xxkm_yyyy_doy_FNL_v03.0.nc
xx = 40 or 70, yyyy = 4-digit year, doy= 3-digit day of year.

2. Monthly Averages

- **Pathname:** /smap/SSS/V03.0/FINAL/L3/monthly/xxkm/yyyy/
- **Filename:** RSS_smmap_SSS_L3_monthly_xxkm_yyyy_mm_FNL_v03.0.nc
xx = 40 or 70, yyyy = 4-digit year, mm= 2-digit month of year.

3. Monthly Rain-Filtered (RF) Averages

- **Pathname:** */smap/SSS/V03.0/FINAL/L3/monthly_RF/xxkm/yyyy/*
- **Filename:** *RSS_smap_SSS_L3_monthly_RF_xxkm_yyyy_mm_FNL_v03.0.nc*
xx = 40 or 70, yyyy = 4-digit year, mm= 2-digit month of year.

7.2.2 Global Attributes

- **first_orbit** (4-byte integer): the 1st rev that is used in the L3 time averaging.
- **last_orbit** (4-byte integer): the last rev that is used in the L3 time averaging.
- **start_time_of_product_interval** (8-byte real): seconds of start time of product interval since 2000-01-01 00:00:00 UTC.
- **end_time_of_product_interval** (8-byte real): seconds of end time of product interval since 2000-01-01 00:00:00 UTC.

7.2.3 Grid and Dimensions

All L3 files are provided on a uniform 0.25°x0.25° rectangular Earth grid.

The **longitude** varies between 0° and 360° in **nxdim = 1440** uniform 0.25° increments. The longitudinal interval midpoints are: 0.125°, 0.375°, ...359.875°.

The **latitude** varies between -90° and +90° in **nydim = 720** uniform 0.25° increments. The latitudinal interval midpoints are: -89.875°, -89.8625°, ..., +89.875°.

The **time** corresponds to the center of the product time interval.

7.2.4 Variables

- **nobs** (4-byte integer, array size = [nxdim, nydim]): number of L2C observations that are averaged into L3 grid cell.
- **sss_smap** (4-byte float, array size = [nxdim, nydim]): SMAP sea surface salinity. units: PSU.
- **sss_ref** (4-byte float, array size = [nxdim, nydim]): HYCOM reference sea surface salinity. units: PSU.
- **gland** (4-byte float, array size = [nxdim, nydim]): land fraction within footprint weighted by antenna gain pattern. range: [0.0, 1.0].
- **gice** (4-byte float, array size = [nxdim, nydim]): sea ice fraction within footprint weighted by antenna gain pattern. range: [0.0, 1.0].
- **surtep** (4-byte float, array size = [nxdim, nydim]): ancillary sea surface temperature from CMC. units: Kelvin.
- **sss_argo** (4-byte float, array size = [nxdim, nydim]): ARGO Scripps sea surface salinity. units: PSU. This field is only present in the rain-filtered (RF) monthly product (section 4.2).